CROATICA CHEMICA ACTA
CCACAA, ISSN 0011-1643, e-ISSN 1334-417X
Croat. Chem. Acta **84** (2) (2011) 251–257.
CCA-3472

Original Scientific Article

Attraction between Like Charged Surfaces Mediated by Uniformly Charged Spherical Colloids in a Salt Solution†

Sylvio May[a] and Klemen Bohinc[b,*]

[a]*Department of Physics, North Dakota State University, Fargo ND, 58108-6050, USA*
[b]*Faculty of Health Sciences, University of Ljubljana, SI-1000 Ljubljana, Slovenia*

RECEIVED JANUARY 15, 2011; REVISED JUNE 27, 2011; ACCEPTED JULY 7, 2011

Abstract. Like-charged macromolecules repel in electrolyte solutions that contain small (*i.e.* point-like) monovalent co- and counterions. Yet, if the mobile ions of one species are spatially extended instead of being point-like, the interaction may turn attractive. This effect can be captured within the mean-field Poisson-Boltzmann framework if the charge distribution within the spatially extended ions is accounted for. This has been demonstrated recently for rod-like ions. In the present work, we consider an electrolyte solution that is composed of monovalent point-like salt ions and uniformly charged spherical colloids, sandwiched between two planar like-charged surfaces. Minimization of the mean-field free energy yields an integral-differential equation for the electrostatic potential that we solve numerically within the linear Debye-Hückel limit. The free energy, which we calculate from the potential, indeed predicts attractive interactions for sufficiently large spherical colloids. We derive an approximate analytical expression for the critical colloid size, above which attraction between like-charged surfaces starts to emerge. (doi: 10.5562/cca1824)

Keywords: Poisson-Boltzmann, ionic interactions, electrostatics, colloids, electrolyte

INTRODUCTION

Interactions between like-charged macromolecules in electrolyte solutions are of fundamental importance in biological and biotechnological systems. They can be attractive in the presence of di- or multivalent ions.[1] For example, divalent diamin ions induce aggregation of rod-like M13 viruses,[2] divalent barium ions mediate network formation in actin solutions,[3] and divalent counterions are able to induce condensation of DNA.[4,5] Multivalent ions that are spatially extended usually show a strong tendency to induce aggregation of like-charged macroions. This is observed for positively charged colloids that condense DNA[6] or for DNA that induces attraction between cationic lipid membranes.[7]

The attraction between like-charged surfaces in the presence of multivalent ions cannot be explained by the classical mean-field Poisson-Boltzmann (PB) theory. In order to predict attraction, charge-charge correlations must be accounted for. One may generally distinguish correlations between different multivalent ions from correlations between the spatially separated charges within a single multivalent ion. We refer to these cases as *inter-ionic* and *intra-ionic* correlations. The former case - especially accounting for correlations when the multivalent ions are point-like - has attracted considerable interest in the past.[8–13] The latter case, *i.e.* accounting for the connectivity of the individual charges within a given spatially extended ion, has received less attention. An example are polyelectrolytes that mean-field electrostatics predicts to mediate attraction if the connectivity of the polymer segments is accounted for.[14] A considerably simpler system is that of rod-like ions where two elementary charges are connected by a stiff rod. Here too, mean-field electrostatics is able to predict attraction if the intra-ionic correlations (*i.e.*, the connectivity between the two charges of each rod-like molecule) are included into the Poisson-Boltzmann formalism.[15–18] This extended Poisson-Boltzmann model predicts a *bridging mechanism*[19] as the structural motif that leads to attraction and eventually to a finite equilibrium distance between two like-charged surfaces. We note that these theoretical predictions are confirmed by Monte Carlo simulations.[16,18,20] The analysis of the system was also extended to the intermediate and strong coupling regimes, where inter-ionic correlations alone can lead to an attraction between the like-charged surfaces.[21]

† This article belongs to the Special Issue *Chemistry of Living Systems* devoted to the intersection of chemistry with life.
* Author to whom correspondence should be addressed. (E-mail: klemen.bohinc@zf.uni-lj.si)

In the present work, we consider an additional system of spatially extended ions, namely spherical colloids that carry a uniform surface charge density. Specifically, we formulate an extended Poisson-Boltzmann model for a mixture of point-like monovalent salt ions and uniformly charged spherical colloids, sandwiched between two extended like-charged surfaces. Our model is a mean-field approach in the sense that correlations between different ions will be neglected. Yet, intra-ionic correlations (*i.e.*, the connectivity of the charges within each spherical colloid) are accounted for accurately. We focus on the Debye-Hückel regime where the charge densities on both the extended planar surfaces and on the surfaces of the spherical colloids are small. The resulting integral differential equation was solved numerically. It is demonstrated that attraction between like-charged surfaces arises above a critical colloid size. We present an approximative analytical expression for this critical size.

THEORY

We consider an aqueous solution that contains a mixture of negatively charged spherical colloids (all of radius *R*) and monovalent point-like salt ions of positive and negative charges. All ions (colloids and salt ions) are mobile, and they are present with bulk concentrations n_0 (for the spheres), n_+^0 (for the positively charged salt ions), and n_-^0 (for the negatively charged salt ions). We assume each spherical colloid carries Z elementary charges that are uniformly distributed over the sphere's surface area. Overall charge neutrality in the bulk then requires

$$n_+^0 = n_-^0 + Z n_0 \,. \tag{1}$$

We also assume that the aqueous solution contains two uniformly charged planar surfaces of large lateral area A, located perpendicular to the *x*-axis of a Cartesian coordinate system at positions $x = 0$ and $x = D$. Translational invariance of the system along the *y* and *z* directions of the Cartesian coordinate system then implies all average system properties to depend only on x (but not on y and z). The two planar surfaces are both positively charged; their surface charge densities σ are identical. Figure 1 shows a schematic representation of the two like-charged surfaces that sandwich the electrolyte with its salt ions and charged spheres; bulk part of the aqueous solution is also present but is not shown.

Clearly, the presence of the charged planar surfaces induces local changes in the concentration of all involved mobile ions. We denote the local concentrations of the positively and negatively charged salt ions by $n_+ = n_+(x)$ and $n_- = n_-(x)$, respectively. The local concentration of the spherical colloids is denoted by

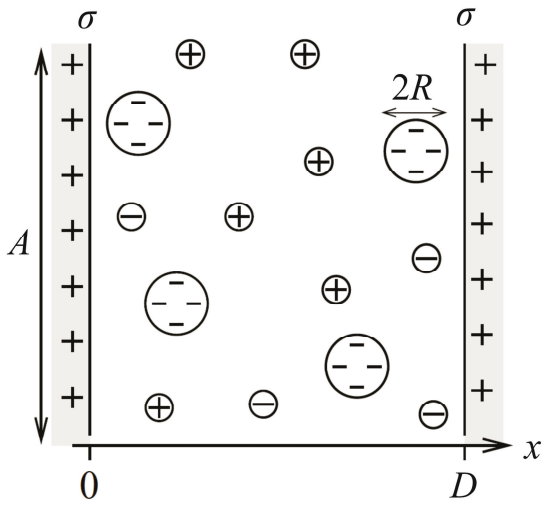

Figure 1. Schematic illustration of two like-charged planar surfaces (located at positions $x = 0$ and $x = D$, each of lateral area A and with surface charge density σ), embedded in an aqueous solution that contains negatively charged spherical colloids and small (point-like) monovalent salt ions of positive and negative charges. All spherical colloids have radius R, with Z negative charges ($Z = 4$ in our illustration) uniformly distributed over the surface of the colloid. The overall system (the planar surfaces together with the sandwiched electrolyte) is electrically neutral.

$n = n(x)$; here x refers to the respective centers of the spheres.

In our description of the electrolyte we neglect inter-ionic correlations (but, as pointed out below, we do account for the intra-ionic correlations of the Z charges within each spherical ion). In this respect our model is a mean-field approach that allows us to express the Helmholtz free energy, measured in units of the surface area A and thermal energy $k_B T$ (here k_B is Boltzmann's constant and T the absolute temperature) as

$$\frac{F}{A k_B T} = \frac{1}{8\pi l_B} \int_0^D \Psi'^2 \,\mathrm{d}x + \int_0^D \left[n \ln \frac{n}{n_0} - (n - n_0) + n_+ \ln \frac{n_+}{n_+^0} - (n_+ - n_+^0) \right] \mathrm{d}x + \int_0^D \left[n_- \ln \frac{n_-}{n_-^0} - (n_- - n_-^0) \right] \mathrm{d}x + \int_0^D n\, U(x)\,\mathrm{d}x, \tag{2}$$

where l_B is the Bjerrum length, $\Psi(x)$ is the dimensionless electrostatic potential, and the prime denotes the derivative with respect to x. Recall that the Bjerrum length corresponds to the distance $l_B = e^2/(4\pi\varepsilon\varepsilon_0 k_B T)$ at which the electrostatic interaction energy of two elementary charges *e* equals $k_B T$. In water, where the permittivity is $\varepsilon \approx 80$ times larger than in free space (where $\varepsilon_0 = 8.85 \times 10^{-12}\,\mathrm{As/(Vm)}$) one finds $l_B \approx 0.7$

nm. Recall also that the dimensionless electrostatic potential is related to the electrostatic potential Φ through $\Psi = e\Phi / k_{\mathrm{B}}T$. Hence, the first term in Eq. (2) represents the total electrostatic energy of the system. The remaining terms account for all non-electrostatic interactions; the first of these contains the mixing entropy contributions of the spherical colloids and salt ions. All mixing entropy contributions are assumed to be ideal. Strictly, one should account for the steric size and shape of the spherical colloids. But below we will only be interested in the limiting (Debye-Hückel) case of small potentials (implying small concentrations of all ions) where the ideal mixing approximation becomes valid. We note that in contrast to analogous models for rod-like ions[16] uniformly charged spherical ions are radially symmetric and thus do not entail an additional orientational entropy contribution to *F*. The last non-electrostatic interaction term in Eq. (2) (*i.e.*, the final integral in Eq. (2)) introduces an external potential $U(x)$ that we employ to model the steric interaction of the spherical colloids with the two planar surfaces. Specifically, to ensure that the colloids cannot penetrate into the planar surfaces we chose $U = 0$ for $R \le x \le D - R$ and $U \to \infty$ otherwise. With this, the centers of the spherical ions are confined to positions $R \le x \le D - R$.

In thermal equilibrium the free energy F adopts its minimum with respect to the local concentrations n_+, n_-, and n. To carry out the minimization we employ Poisson's equation $\Psi''(x) = -4\pi l_{\mathrm{B}}\rho(x)/e$, where the local volume charge density

$$\rho(x) = en_+(x) - en_-(x) - eZ\left\langle n(x-s)\right\rangle_s \tag{3}$$

at position x contains contributions from the point-like salt ions $(en_+ - en_-)$ as well as from the spherical colloids. In Eq. (3) we have introduced the averaging $\left\langle f\right\rangle_s$ of any given physical quantity $f(s)$ according to

$$\left\langle f\right\rangle_s = \frac{1}{2R}\int_{-R}^{R} f(s)\,\mathrm{d}s, \tag{4}$$

where the index s refers to the integration variable. Hence the term $\left\langle n(x-s)\right\rangle_s$ in Eq. (3) accounts for all positions of the spherical colloids, ranging from $x - R$ to $x + R$, that contribute to the charge density at position x. Based on Eqs. (2–4) one can calculate from the vanishing first variation $\delta F(n, n_+, n_-) = 0$ the equilibrium distributions

$$n(x) = n_0\,\mathrm{e}^{Z\left\langle \Psi(x+s)\right\rangle_s - U(x)}, \tag{5}$$

$$n_+(x) = n_+^0\,\mathrm{e}^{-\Psi(x)},$$

$$n_-(x) = n_-^0\,\mathrm{e}^{+\Psi(x)}.$$

Note that for n_+ and n_- we find the familiar Boltzmann distributions for point-like ions. The distribution n for the spherical colloids depends on the dimensionless electric potential Ψ in the entire region from $x - R$ to $x + R$. Hence, the distribution function is non-local.

Inserting the volume charge density (Eq. (3)) into Poisson's equation and using the distribution functions in Eq. (5) yields the following integral-differential equation

$$l_D^2\Psi''(x) = \sinh\Psi(x) - \frac{\alpha}{2}\left[\mathrm{e}^{\Psi(x)} - \left\langle \mathrm{e}^{Z\left\langle \Psi(x+s-\bar{s})\right\rangle_s - U(x-\bar{s})}\right\rangle_{\bar{s}}\right] \tag{6}$$

where the length l_D is defined through $l_{\mathrm{D}}^2 = 1/(8\pi l_{\mathrm{B}} n_+^0)$. Moreover, $\alpha = Zn_0/n_+^0$ is the fraction between the negative charges that all colloids contain and all negative charges in the system (point-like anions and colloid charges). Note that l_{D} and α have a simple physical interpretation: For $\alpha = 0$ all mobile ions are point-like, and l_{D} would be the Debye screening length of that symmetric 1:1 electrolyte. For $\alpha = 1$ all negative charges in the system are bound to the colloids; the bulk electrolyte then contains only negatively charged colloids and the corresponding point-like (monovalent and positively charged) counterions. Intermediate values of α (with $0 < \alpha < 1$) specify the fraction of negative charges in the bulk electrolyte that are attached to the colloids. Hence, increasing α at fixed Z translates into rearranging initially point-like monovalent anions as surface charges of spherical colloids.

Formally, Eq. (6) corresponds to the nonlinear Poisson-Boltzmann equation, generalized to account for the presence of uniformly charged spherical colloids with radius R and valence Z. However, because we have not accounted properly for the conformational entropy of the hard-sphere fluid of colloids (which is sandwiched between two rigid surfaces) it is appropriate to only consider the Debye-Hückel limit where the potential $\Psi << 1$ and the concentration n is small. In this case, the integral-differential equation (Eq. (6)) can be linearized which results in

$$\begin{aligned} l_D^2\Psi''(x) = {} & \Psi(x)\left(1 - \frac{\alpha}{2}\right) - \frac{\alpha}{2} + \\ & \frac{\alpha}{2}\left\langle\left(1 + Z\left\langle \Psi(x+s-\bar{s})\right\rangle_s\right)\mathrm{e}^{-U(x-\bar{s})}\right\rangle_{\bar{s}}. \end{aligned} \tag{7}$$

The integral-differential equation (7) has to be solved subject to the boundary conditions

$$\Psi'(0) = -4\pi l_{\mathrm{B}}\frac{\sigma}{e} \qquad \Psi'(D) = +4\pi l_{\mathrm{B}}\frac{\sigma}{e}, \tag{8}$$

where we recall that σ denotes the surface charge density on each of the two planar surfaces.

For sufficiently small spherical ions we can perform a series expansion of the last term in Eq. (7) with respect to the radius R up to fourth order. This results in the fourth-order ordinary differential equation,

$$\frac{2}{45}R^4\Psi^{(4)}+\left(\frac{R^2}{3}-\frac{2l_D^2}{\alpha Z}\right)\Psi^{(2)}+\left(\frac{2}{\alpha Z}-\frac{1}{Z}+1\right)\Psi=0 \qquad (9)$$

where $\Psi^{(i)}(x)$ denotes the i-th derivative of Ψ with respect to x. With regard to finding appropriate boundary conditions for Eq. (9) we note that our choice of $U(x)$ renders the factor $\mathrm{e}^{-U(x-\bar{s})}$ in Eq. (7) non-analytic for small R. Only in the limit $R\to 0$ is the factor $\mathrm{e}^{-U(x-\bar{s})}=1$ and thus does not contribute to the expansion in Eq. (9). One may set $\mathrm{e}^{-U(x-\bar{s})}=1$ even for finite radius, but this neglects the exclusion of the sphere centers from the regions close to the planar surfaces and is an unjustified approximation. Hence, below (see Eq. (16)) we will use Eq. (9) to only predict the critical colloid radius above which attractive interactions between like-charged surfaces emerge (rather than to explicitly solve Eq. (9)). The emergence of attractive interactions is not affected by the boundary conditions of Eq. (9).

The equilibrium free energy of the system is obtained by inserting the linearized (valid for $\Psi<<1$) equilibrium distributions (Eqs. (5)) into Eq. (2). This results in

$$\frac{F}{Ak_BT}=\frac{\sigma}{e}\Psi(0)+2Rn_0+\frac{1}{2}\int_0^D\Psi(x)\left[\,n_+^0-n_-^0-Zn_0\left\langle\mathrm{e}^{-U(x-s)}\right\rangle_s\right]\mathrm{d}x, \qquad (10)$$

where the second term $(2Rn_0)$ is constant (*i.e.*, independent of the separation D between the planar surfaces) and irrelevant for further considerations.

In the limit of $R\to 0$ the last term in Eq. (10) vanishes because of the overall charge neutrality in the bulk; see Eq. (1). Thus, in this limit ($R\to 0$) the free energy

$$\frac{F}{Ak_BT}=\frac{\sigma}{e}\Psi(0) \qquad (11)$$

becomes determined by the electrostatic surface potential $\Psi(0)$, which can be calculated immediately from solving the differential equation (9). For the free energy we obtain

$$\frac{F}{Ak_BT}=4\pi l_B\left(\frac{\sigma}{e}\right)^2\cdot\frac{1}{\lambda}\cdot\coth\frac{\lambda D}{2}, \qquad (12)$$

where

$$\lambda=\frac{1}{l_D}\sqrt{1+\frac{\alpha}{2}(Z-1)} \qquad (13)$$

is the inverse Debye screening length corresponding to this mixed-valency electrolyte (valencies 1 and Z) of point-like ions, sandwiched between two like-charged planar surfaces. Eq. (12) is the classical Debye-Hückel free energy expression; it predicts repulsion between the two like-charged surfaces.

RESULTS AND DISCUSSION

We first consider a system where the separation D between the planar surfaces equals four times the diameter of the spherical colloids; $D=8R$. We assume each spherical colloid has 5 charges attached to its surface (hence $Z=5$). Figure 2 displays the dimensionless electrostatic potential Ψ between the two surfaces as function of the x-coordinate. It is convenient to scale all distances by the length l_D. That is we define the dimensionless lengths $\bar{x}=x/l_D$, $\bar{D}=D/l_D$ and $\bar{R}=R/l_D$. The different curves in Figure 2 correspond to different choices of the parameter α. As mentioned above this parameter has an intuitive physical interpretation: it specifies the total fraction of all negative charges (monovalent salt ions plus spherical colloids) that are attached to the colloids. As Figure 2 shows, increasing α has a large influence not only on the magnitude of the potential $\Psi(x)$ but also on its qualitative behavior. For small α the system contains few colloids, and the electrostatic potential monotonically decreases with increasing distance from the charged surface. Upon increasing α above a certain value we find the electrostatic potential to exhibit damped oscillations (curves (a) and (b) in the left diagram of Figure 2).

In the limit of infinitesimal small radius R the potential converges to the classical Debye-Hückel result for point-like ions

$$\Psi(x)=\frac{2pl_D}{\lambda}\cdot\frac{\cosh(\lambda x)+\cosh(\lambda D-\lambda x)}{\sinh(\lambda D)} \qquad (14)$$

where we have defined the quantity $p=2\pi l_B l_D\sigma/e$ as a convenient measure for the surface charge density. The inverse Debye screening length λ is given in Eq. (13). For $\alpha=0$ we have $\lambda=1/l_D$, and Eq. (14) recovers our numerical calculations (curves (d) in the left and right diagrams of Figure 2). Upon increasing the (scaled) radius of the spherical colloids beyond a critical value R^c (which we calculate below in Eq. (16)) the potential becomes non-monotonic. The oscillations in $\Psi(x)$ are accompanied

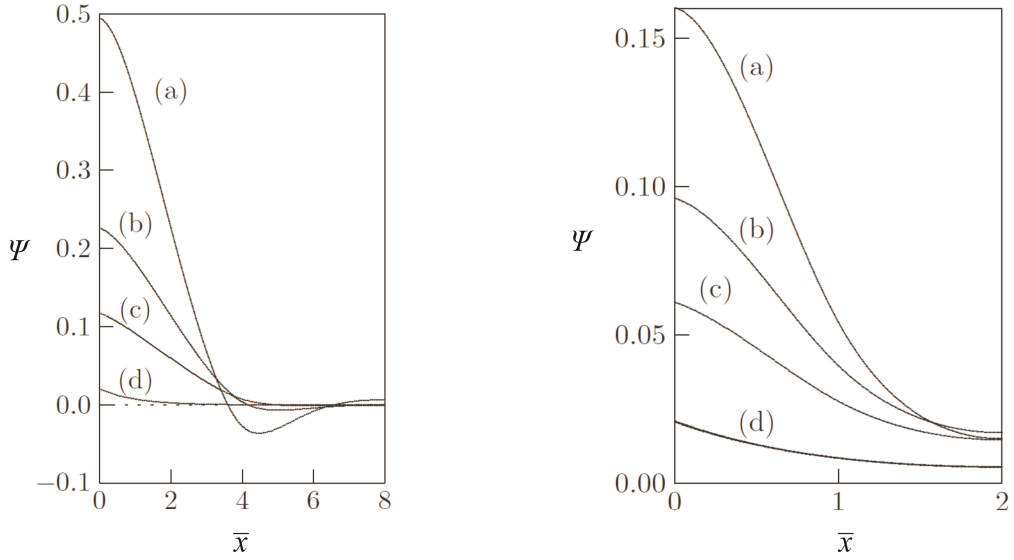

Figure 2. Dimensionless electrostatic potential as a function of the scaled distance $\bar{x}$ away from the charged plate. The left diagram refers to $\bar{R} = 2$ and $\bar{D} = 16$. The right diagram refers to $\bar{R} = 0.5$ and $\bar{D} = 4$. The four curves in each diagram correspond to $\alpha = 1$ (a), $\alpha = 0.5$ (b), $\alpha = 0.25$ (c) and $\alpha = 0$ (d). The remaining parameters are $Z = 5$ and $p = 0.01$.

by overcharging where the charge of the spherical colloids over-compensates the charges on the planar surfaces. This is a typical signature for the emergence of attractive interactions between the like-charged surfaces.

Figure 3 displays (scaled) concentrations of the spherical colloids n / n_0, of the positively charged monovalent ions n_+ / n_0, and of the negatively charged monovalent ions n_- / n_0, all as function of the scaled distance $\bar{x}$ away from the charged planar surface. We again use $\bar{R} = 2$, $Z = 5$, $\bar{D} = 16$, and two different values for α in the left and right diagrams (corresponding to curves (a) and (b) in the left diagram of Figure 2). Because the separation between the charged surfaces in Figure 3 is large compared to the radius of the colloids, we recover bulk conditions midway between the two surfaces (*i.e.* $n_+(\bar{x}) \approx 5\, n(\bar{x})$ at $\bar{x} = 8$ in the left diagram of Figure 3). Close to the surfaces, the concentration of colloids is increased, most strongly in the limit $\alpha = 1$ (left diagram in Figure 3). Let us discuss if the colloid concentration remains in the dilute regime. In the bulk the condition is $(4/3)\pi R^3 n_0 << 1$. Using the definitions for α and l_D, this can be written as

$$\frac{l_D}{l_B} << \frac{6Z}{\alpha \bar{R}^3} \tag{15}$$

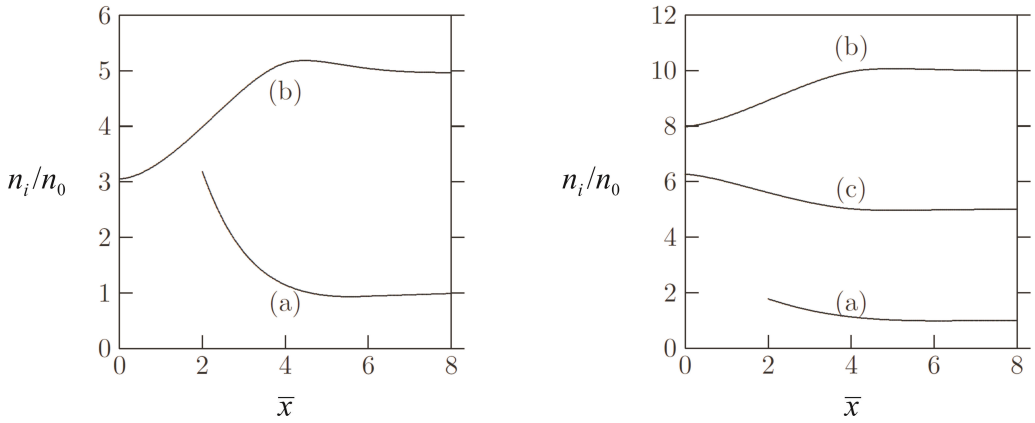

Figure 3. Scaled concentrations of negatively charged spherical colloids n / n_0 (a), positively charged point-like monovalent ions n_+ / n_0 (b) and negatively charged point-like monovalent ions n_- / n_0 (c) as a function of the scaled distance away from the charged plate. Left and right diagrams refer to $\alpha = 1$ and $\alpha = 0.5$, respectively. The remaining parameters are $Z = 5$, $p = 0.01$, $\bar{R} = 2$ and $\bar{D} = 16$. Note that the left and right diagrams correspond to, respectively, curves (a) and (b) in the left diagram of Figure (2).

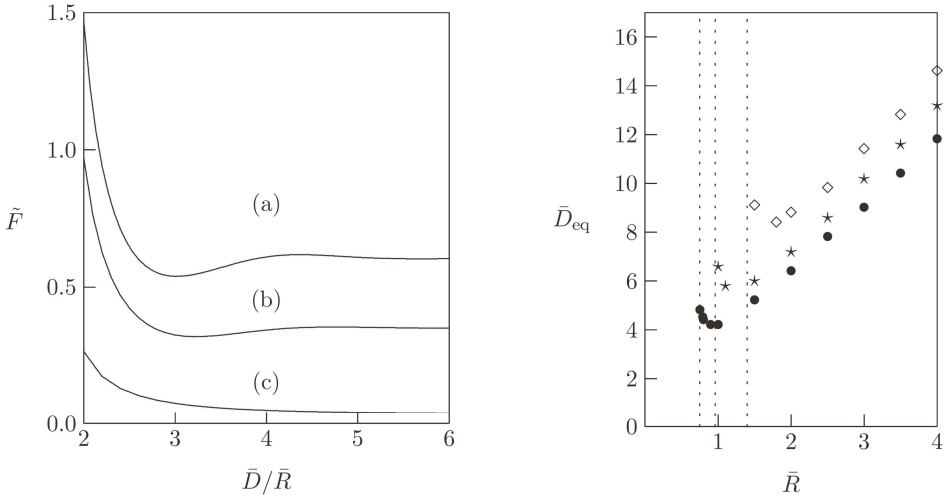

Figure 4. Left diagram: Free energy $\tilde{F} = F/(Zn_0 Ak_B T l_D) - 2\bar{R}/Z$ as a function of the plate separation for $\bar{R} = 3$ (a), $\bar{R} = 2$ (b), and $\bar{R} = 0.5$ (c), all calculated for $Z = 5$, $\alpha = 1$ and $p = 0.01$. Right diagram: The (scaled) equilibrium distance $\bar{D}_{eq}$ between the charged surfaces as a function of the colloid radius $\bar{R}$. The vertical broken lines represent the numerically obtained critical colloid radius. The bullets correspond to $\alpha = 1$ and $Z = 5$, the stars correspond to $\alpha = 0.5$ and $Z = 5$ whereas the diamonds correspond to $\alpha = 0.5$ and $Z = 2$. The remaining parameter is $p = 0.01$.

For our specific conditions in the left diagram of Figure 3 ($Z = 5$, $\alpha = 1$, $l_B = 0.7\,\mathrm{nm}$, and $\bar{R} = 2$) Eq. (15) implies $l_D << 2.6\,\mathrm{nm}$ or, equivalently, $n_+^0 >> 10\,\mathrm{mmol\,dm^{-3}}$. To account for the three-fold increase of the colloid concentration at the surface $l_D << 2.6\,\mathrm{nm}/3 \approx 0.9\,\mathrm{nm}$. This leaves only considerably larger concentrations than 0.1 mmol dm^{-3} for n_+^0. In this case the packing fraction of spheres $4\pi R^3 n_0/3$ is approximately 0.4. For $\alpha = 0.5$ (right diagram of Figure 3) the condition for a dilute solution is $l_D << 5.2\,\mathrm{nm}$ or, equivalently, $n_+^0 >> 3.3\,\mathrm{mmol\,dm^{-3}}$. Here, the concentration of colloids at the surface roughly doubles as compared to the bulk (see curve (a) in the right diagram of Figure 3), leaving a much wider concentration range, $n_+^0 >> 10\,\mathrm{mmol\,dm^{-3}}$, that ensures dilute conditions everywhere in the system.

The free energy (see Eq. (10)) as a function of the (scaled) distance between two like-charged surfaces is shown in the left diagram of Figure 4. Results for three different radii of the spherical colloids are presented. For small radius ($\bar{R} = 0.5$ in the left diagram of Figure 4) the free energy monotonously decreases with increasing plate separation $\bar{D}$. That is, the interaction is always repulsive. For sufficiently large radius ($\bar{R} = 2$ and $\bar{R} = 3$ in the left diagram of Figure 4) the free energy passes through one (or several) minima. The closest minimum position is somewhat larger than the diameter of the spherical colloids, implying that the colloids contribute to the neutralization of both planar surfaces at the same time. Hence, they bridge between the two surfaces, similarly as polyelectrolytes[14,19] or stiff rod-like ions[16] do. Their intra-ionic correlations (*i.e.*, the connectivity between the individual charges in each colloid) renders spatially extended ions generally able to induce attractive interactions between like-charged surfaces through a bridging mechanism.

The (scaled) equilibrium separation $\bar{D}_{eq}$ between the planar surfaces is shown in the right diagram of Figure 4 as a function of the (scaled) colloid radius $\bar{R}$. The valency Z has small influence on the equilibrium distance $\bar{D}_{eq}$ (see Figure 4, right diagram). Note that $\bar{D}_{eq}$ refers to the smallest equilibrium separation $\bar{D}$ between the planar surfaces. For sufficiently large $\bar{R}$ the equilibrium distance is about 1.5 times larger than the diameter $2\bar{R}$ of the spherical colloids. We point out that a finite equilibrium distance $\bar{D}_{eq}$ starts to exist only above a critical colloid radius $R > R^c$. An approximative expression for the critical colloid radius R^c is

$$R^c = l_D \sqrt{\frac{6}{\alpha Z}} \tag{16}$$

This expression is approximative because it follows from Eq. (9), which was derived for the limit of small *R*. The characteristic equation corresponding to Eq. (9) defines two characteristic lengths. One of these lengths vanishes at $\bar{R} = \sqrt{6/(\alpha Z)}$. This corresponds to the vanishing of the prefactor $(R^2/3) - (2l_D^2)/(\alpha Z)$ in front of Ψ'' in Eq. (9). Let us calculate for which of the curves in the left diagram of Figure 2 a finite equilibrium distance is predicted by Eq. (16): For $\bar{R} = 2$ and $Z = 5$ we obtain $\alpha = 6/(\bar{R}^2 Z) = 0.3$. Hence, curves (a) and (b) in the left diagram of Figure 2 are non-monotonic. Similarly for the left diagram of Figure 4,

the (scaled) critical radius is $\overline{R}^c = R^c / l_D = \sqrt{6/(\quad)} = \sqrt{6/5} \approx 1.1$. Hence, curves (a) and (b) but not (c) are predicted to be nonmonotonic. This all agrees with our results from numerically solving Eq. (7). In fact, the right diagram of Figure 4 suggests that $\overline{R}^c$ in Eq. (16) reasonably well predicts the critical colloid size of the present Debye-Hückel approach.

In summary, we have developed a modified linearized Poisson-Boltzmann model for an electrolyte that contains besides point-like monovalent ions also uniformly charged spherical colloids, sandwiched between two parallel like-charged surfaces. Our results clearly indicate the possibility of condensation (*i.e.*, resulting from attractive interactions) between the spherical colloids and the extended, like-charged planar surfaces. The attractiveness of the interaction is the result of intra-ionic correlations introduced through the uniform surface charge density of the (spatially extended) spherical colloids.

Acknowledgements. This work was supported by NSF through grant DMR-0605883. The authors also acknowledge support by the Slovenian Research Agency through grant No. BI-US/11-12-046.

REFERENCES

1. D. F. Evans and H. Wennerström, *The colloidal domain, where physics, chemistry, biology and technology meet*, 2nd ed., VCH Publishers, New York, 1994.
2. J. C. Butler, T. Angelini, J. X. Tang, and G. C. L. Wong, *Phys. Rev. Lett.* **91** (2003) 028301.
3. T. E. Angelini, H. Liang, W. Wriggers, and G. C. L. Wong, *Proc. Natl. Acad. Sci. U S A* **100** (2003) 8634.
4. V. A. Bloomfield, *Curr. Opin. Struct. Biol.* **6** (1996) 334.
5. V. Teif, *Biophys. J.* **89** (2005) 2574.
6. W. M. Gelbart, R. Bruinsma, P.A. Pincus, and V. A. Parsegian, *Physics today* **53** (2000) 38.
7. J. O. Rädler, I. Koltover, T. Salditt, and C. R. Safinya, *Science* **275** (1997) 810.
8. J. G. Kirkwood and J. B. Shumaker, *Proc. Natl. Acad. Sci. USA* **38** (1952) 863.
9. F. Oosawa, *Biopolymers* **6** (1986) 1633.
10. A. G. Moreira and R. R. Netz, *Phys. Rev. Lett.* **87** (2001) 078301.
11. Y. Levin, *Rep. Prog. Phys.* **65** (2002) 1577.
12. R. Kjellander and S. Marcelja, *J. Phys. France* **49** (1988) 1009.
13. R. Kjellander, and S. Marcelja, *J. Phys. Chem. B* **113** (1988) 2160.
14. I. Borukhov, D. Andelman, and H. Orland, *J. Phys. Chem. B* **103** (1999) 5042.
15. K. Bohinc, A. Iglic, and S. May, *Europhys. Lett.* **68(4)** (2004) 494.
16. S. May, A. Iglic, J. Rešcic, S. Maset, and K. Bohinc, *J. Chem. Phys. B* 112 (2008) 1685.
17. S. Maset and K. Bohinc, *J. Phys. A: Math. Theor.* **40** (2007) 11815.
18. S. Maset, J. Rešcic, S. May, J. I. Pavlic, and K. Bohinc, *J. Phys. A: Math. Theor.* **42** (2009) 105401.
19. R. Podgornik, *J. Polym. Sci. Part B-Polym. Phys.* **42** (2004) 3539.
20. Y. W. Kim, J. Yi, and P. A. Pincus, *Phys. Rev. Lett.* **101** (2008) 208305.
21. M. M. Hatlo, K. Bohinc, and L. Lue, *J. Chem. Phys.* **132** (2010) 114102.